

# Bounds on the spectra of Schur complements of large H-TFETI-DP clusters for 2D Laplacian

Zdeněk Dostál<sup>1,2</sup> | David Horák<sup>1</sup> | Tomáš Brzobohatý<sup>2</sup> | Petr Vodstrčil<sup>1</sup>

<sup>1</sup>Department of Applied Mathematics,  
 Faculty of Electrical Engineering and  
 Computer Science, VŠB-Technical  
 University of Ostrava, Ostrava, Czech  
 Republic

<sup>2</sup>IT4Innovations, National  
 Supercomputing Center, VŠB-Technical  
 University of Ostrava, Ostrava, Czech  
 Republic

## Correspondence

Zdeněk Dostál, Department of Applied Mathematics, Faculty of Electrical Engineering and Computer Science, VŠB-Technical University of Ostrava, Ostrava, Czech Republic.  
 Email: zdenek.dostal@vsb.cz

## Funding information

Ministry of Education, Youth, and Sport of the Czech Republic, Grant/Award Number: LQ1602; Large Infrastructures for Research, Experimental Development and Innovations project IT4Innovations National Supercomputing Center, Grant/Award Number: LM2015070

## Abstract

Bounds on the spectrum of Schur complements of subdomain stiffness matrices of the discretized Laplacian with respect to interior variables are important in the convergence analysis of finite element tearing and interconnecting (FETI)-based domain decomposition methods. Here, we are interested in bounds on the regular condition number of Schur complements of “floating” clusters, that is, of matrices comprising the Schur complements of subdomains with prescribed zero Neumann conditions that are joined on the primal level by edge averages. Using some known results, angles of subspaces, and known bounds on the spectrum of Schur complements associated with square domains, we give bounds on the regular condition number of the Schur complement of some “floating” clusters arising from the discretization and decomposition of 2D Laplacian on domains comprising square subdomains. The results show that the condition number of the cluster defined on a fixed domain decomposed into  $m \times m$  square subdomains joined by edge averages increases proportionally to  $m$ . The estimates are compared with numerical values and used in the analysis of H-FETI-DP methods. Though the research has been motivated by an effort to extend the scope of scalability of FETI-based solvers to variational inequalities, the experiments indicate that H-TFETI-DP with large clusters can be useful for the solution of huge linear elliptic problems discretized by sufficiently regular grids.

## KEY WORDS

bounds on spectrum, hybrid FETI, Schur complement

## 1 | INTRODUCTION

Variants of the finite element tearing and interconnecting (FETI) methods introduced by Farhat and Roux<sup>1,2</sup> belong to the most powerful methods for massively parallel solution of large discretized elliptic partial differential equations. The basic idea is to decompose the domain into subdomains which are joined by Lagrange multipliers and then to eliminate the primal variables to get a small global problem and a number of local problems that can be solved in parallel. After Farhat et al.<sup>3</sup> proved that the condition number of the dual stiffness matrix is uniformly bounded on the subspace defined by the kernels of subdomain stiffness matrices, FETI became the first theoretically supported massively parallel scalable solver for elliptic PDE. The subspace is also called the natural coarse grid. If we apply

FETI to an elliptic variational inequality, it turns out that not only the duality transforms inequality constraints into bound constraints, but that the solution is in the subspace defined by the natural coarse grid. These observations were used for the development of massively parallel scalable algorithms for the solution of elliptic variational inequalities (currently tens of thousands cores for billions of variables<sup>4</sup>). More on FETI methods can be found, for example, in Tosseli and Widlund.<sup>5</sup>

The bottleneck of the original FETI is caused by the dimension of the coarse problem that is proportional to the number of subdomains. The coarse problem is typically solved by a direct solver—its cost is negligible for a small number of subdomains, but it starts to dominate when the number of subdomains is large, currently some tens of thousands subdomains. To overcome the latter limitation and to reduce the dimension of the coarse problem without compromising the number of subdomains, Klawonn et al.<sup>6–8</sup> used the idea of FETI-DP (see, e.g., Farhat et al.<sup>9</sup>) to enforce some constraints on primal level to join groups of subdomains into *clusters* so that the defect of each cluster is the same as that of each of its subdomains. See also Brzobohatý et al.<sup>10,11</sup> or Lee.<sup>12,13</sup> The latter authors use a variant of FETI called TFETI (total FETI) which enforces the Dirichlet conditions by Lagrange multipliers<sup>14</sup> so that all subdomains are floating and their stiffness matrices have a priori known kernels. The methods which combine FETI-DP with TFETI are called H-TFETI-DP (hybrid TFETI).

Both the original FETI-DP and H-FETI-DP were combined with preconditioners and their scalability was proved in the context of preconditioned methods. The preconditioning is a standard tool for the solution of linear problems, but it becomes a complication when we try to apply it to variational inequalities. The reason is that preconditioning turns the bound constraints into more general inequality constraints, excluding the possibility to use specialized quadratic programming solvers.<sup>15</sup> Thus, there is a natural question whether the coarse grid defined by the kernels of clusters is sufficient to get scalable algorithms for contact problems and a good reason to study conditioning of the clusters.

Known results seem to be limited to experimental results by Klawonn and Rheinbach<sup>7</sup> and Lee.<sup>12</sup> Recent qualitative estimates by Vodstrčil et al.<sup>16</sup> assume small (two-by-two subdomains) clusters joined in corners or by edge averages. Here, we extend the results of Reference 16 to larger clusters, prove the relations known so far only from experiments, plug them into the analysis of H-TFETI without preconditioning, and validate the results by numerical experiments. The numerical experiments indicate that the two-level structure of stiffness matrices used by H-TFETI-DP complies well with the hierarchical organization of modern supercomputers and can be useful even for the solution of huge linear elliptic problems discretized by sufficiently regular grids. However, the results are more important for the numerical solution of variational inequalities, as the preconditioning effect is not achieved at the cost of transformation of variables—unpreconditioned H-TFETI-DP preserves bound constraints of the dual QP problems that can be solved by specialized algorithms.<sup>15</sup> The results open a way to extending the scope of scalability of powerful massively parallel algorithms for the solution of variational inequalities.<sup>4</sup>

## 2 | DOMAIN DECOMPOSITION, SUBDOMAINS, AND CLUSTERS

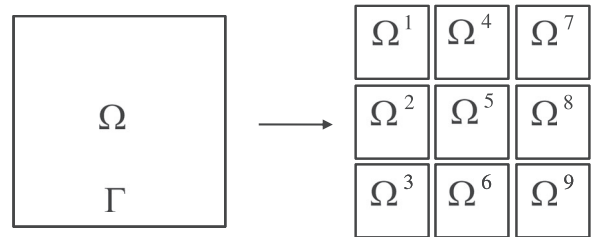
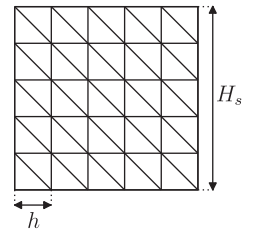
Let us consider a model elliptic problem governed by the Laplacian on the 2D unit square  $\Omega = (0, 1) \times (0, 1)$  with the boundary  $\Gamma$ , such as the Poisson equation

$$\Delta u = f \quad (1)$$

with homogeneous Dirichlet, Neumann, or Signorini conditions. The latter specifies implicitly by inequalities which parts of the boundary are associated with specific classical conditions.<sup>17</sup> For the application of TFETI, let us decompose  $\Omega$  into square subdomains  $\Omega^i$  of the equal side-length  $H_s$  with the boundaries  $\Gamma^i$  as in Figure 1,  $i = 1, \dots, s$ ,  $s = 1/H_s^2$ . In each  $\Omega^i$ , we introduce a regular triangularization with the discretization parameter  $h$  and the pattern depicted in Figure 2. Let  $n_s$  and  $n_e$  denote the number of nodes on the boundary of each subdomain and in the interior of each of its edges, respectively, so that in our case

$$n_s = 4H_s/h \quad \text{and} \quad n_e = H_s/h - 1.$$

We assume matching discretization of subdomains, so the nodes coincide on the interface.

**FIGURE 1** Decomposition of  $\Omega$  into  $3 \times 3$  subdomains**FIGURE 2** Subdomain  $\Omega^i$  and its triangularization

For each subdomain  $\Omega^i$ ,  $i=1, \dots, s$ , we introduce standard finite element linear basis functions and set up local stiffness matrices  $K^i$ , local nodal displacement vectors  $u^i$ , and local load vectors  $f^i$ ,

$$K = \text{diag}(K^1, \dots, K^s), \quad u = \begin{bmatrix} u^1 \\ \vdots \\ u^s \end{bmatrix}, \quad f = \begin{bmatrix} f^1 \\ \vdots \\ f^s \end{bmatrix}.$$

Notice that each local stiffness matrix  $K^i$  is symmetric positive semidefinite with the kernel spanned by the vector

$$r^i = [1, \dots, 1]^T.$$

The solution of the discretized problem (1) can be obtained by the solution of a constrained quadratic programming problem

$$\min \frac{1}{2} u^T Ku - f^T u \quad \text{subject to} \quad B_E u = o \quad \text{and} \quad B_I u \leq o, \quad (2)$$

where  $B_E$  represents the interconnectivity of subdomains and Dirichlet boundary conditions,  $B_I$  enforces the Signorini conditions, and  $o$  denotes zero vector. The matrices  $B_E$  and  $B_I$  can be defined as submatrices of a matrix  $B$  with the column blocks complying with the block structure of  $K$ , that is,

$$B = \begin{bmatrix} B_E \\ B_I \end{bmatrix} = [B_1, \dots, B_s].$$

Both original FETI algorithm (also referred to as FETI1)<sup>1</sup> and TFETI<sup>14</sup> were proposed for linear problems. The idea was to switch to the constrained dual problem in Lagrange multipliers and solve it iteratively with preconditioning by the projector

$$P = I - G^T(GG^T)^{-1}G, \quad G = R^T B^T, \quad R = \text{diag}(r^1, \dots, r^s).$$

The method was later adapted to the solution of variational inequalities.<sup>4,18</sup> In the latter case, the dual problem reads

$$\min \frac{1}{2} \lambda^T F \lambda - d^T \lambda \quad \text{subject to} \quad G \lambda = e \quad \text{and} \quad \lambda_I \geq o, \quad (3)$$

where

$$F = BK^+B^T, \quad d = BK^+f, \quad e = R^T f, \quad \text{and} \quad \lambda = [\lambda_E^T, \lambda_I^T]^T$$

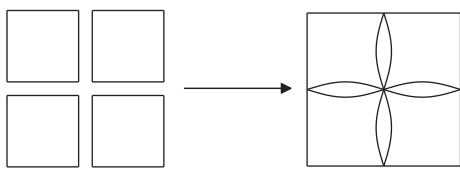


FIGURE 3 Joining of four subdomains in adjacent corners

denote the Lagrange multipliers with the components enforcing the equality and inequality constraints. Recall that if  $A$  is a square matrix, then its generalized inverse  $A^+$  satisfies

$$AA^+A = A.$$

The regular condition number  $\bar{\kappa}(PFP) = \kappa(F|\text{Im}P)$  was shown in Reference 3 to satisfy

$$\bar{\kappa}(PFP) \leq CH/h \quad (4)$$

with a constant  $C$  independent of the decomposition and discretization parameters  $H = H_s$  and  $h$ , respectively. This estimate guarantees an optimal complexity of the method for variational inequalities provided the cost of the action of the projector  $P$  which is used as preconditioner does not dominate the cost of iterations.

To overcome the latter limitation, it is possible to start with the idea by Farhat et al.<sup>19</sup> who proposed to enforce some constraints explicitly. For example, to join four adjacent subdomains in the only common node

$$x \in \overline{\Omega}^i \cap \overline{\Omega}^j \cap \overline{\Omega}^k \cap \overline{\Omega}^\ell,$$

we can transform the nodal variables associated with

$$\tilde{\Omega}^m = \overline{\Omega}^i \times \overline{\Omega}^j \times \overline{\Omega}^k \times \overline{\Omega}^\ell$$

by the expansion matrix  $L^m$  obtained by replacing appropriate four columns of the identity matrix by their sum. Feasible variables  $u^m$  of the cluster are related to global variables  $\tilde{u}^m$  by

$$u^m = L^m \tilde{u}^m$$

and the stiffness matrix  $\tilde{K}^m$  of such cluster in global variables can be obtained by

$$\tilde{K}^m = (L^m)^T \text{diag}(K^i, K^j, K^k, K^\ell) L^m.$$

Moreover, the kernel  $\text{Im}\tilde{R}^m$  of  $\tilde{K}^m$  is only one dimensional, while the dimension of that of  $\text{diag}(K^i, K^j, K^k, K^\ell)$  is four. The cluster resulting from the joining of four subdomains in adjacent corners is depicted in Figure 3.

If we denote by  $L$  the global block diagonal matrix which joins the subdomains in corners, that is, which enforces the same values of the variables associated with a common node, we get the stiffness matrix  $\tilde{K}$  of  $\Omega$  and the constraint matrices  $\tilde{B}_E$  and  $\tilde{B}_I$  in global variables in the form

$$\tilde{K} = L^T K L, \quad \tilde{B}_E = E B_E L, \quad \tilde{B}_I = B_I L, \quad \tilde{R} = L^T R, \quad \tilde{B} = \begin{bmatrix} \tilde{B}_E \\ \tilde{B}_I^T \end{bmatrix},$$

where  $E$  denotes a matrix obtained from the identity matrix by deleting the rows that correspond to zero rows of  $B_E L$ . In this way, we obtain the problem to find

$$\min \frac{1}{2} \lambda^T \tilde{F} \lambda - \tilde{d}^T \lambda \quad \text{subject to} \quad \tilde{G} \lambda = e \quad \text{and} \quad \lambda_I \geq 0, \quad (5)$$

where

$$\tilde{F} = \tilde{B} \tilde{K}^+ \tilde{B}^T, \quad \tilde{K} = \text{diag}(\tilde{K}^1, \dots, \tilde{K}^s), \quad \tilde{G} = \tilde{R}^T \tilde{B}^T, \quad \text{and} \quad \lambda = [\lambda_E^T, \lambda_I^T]^T.$$

The matrix  $\tilde{K}$  is block diagonal because there are no primal constraints on variables of different clusters. Moreover, each  $\tilde{K}^i$ ,  $i = 1, \dots, s$ , can be reordered to get

$$\tilde{K}^i = \begin{bmatrix} \tilde{K}_{RR}^i & \tilde{K}_{RC}^i \\ \tilde{K}_{CR}^i & \tilde{K}_{CC}^i \end{bmatrix}, \quad \tilde{K}_{RR}^i = \text{diag}(K_{RR}^1, \dots, K_{RR}^{s_C}),$$

where  $C$  and  $R$  denote the indices of joined corner and remaining variables, respectively, and  $s_C$  denotes the number of subdomains that are interconnected into the cluster. The vector of Lagrange multipliers  $\lambda$  has components enforcing the inequality constraints and the equality constraints which were left after joining. In this way, we managed to reduce the number of constraints (i.e., the rows of the matrix  $\tilde{G}$ ) by the factor of four, but the regular condition number of  $\tilde{F}$  deteriorated to

$$\bar{\kappa}(\tilde{P}\tilde{F}\tilde{P}) \leq C_1 H \left( 1 + \ln \frac{H}{h} \right) / h, \quad \tilde{P} = I - \tilde{G}^T (\tilde{G}\tilde{G}^T)^{-1} \tilde{G}, \quad (6)$$

with  $C_1 > C$  (see Vodstrčil et al.<sup>16</sup>).

It has been observed that with a standard preconditioning, it is better to join the subdomains by averages, see, for example, Farhat et al.<sup>9</sup> or Klawonn and Widlund,<sup>20</sup> assembling clusters by averages can be found in Klawonn and Rheinbach.<sup>6,7</sup> Here, we are interested what happens without preconditioning. In particular, we show that it is possible to get similar optimality results for H-TFETI as for FETI1, so that the optimality results for the solution of (3) (see, e.g., Dostál and Horák<sup>21</sup> or the book [4, chapter 10]) by TFETI apply also for H-TFETI-based algorithms for (5).

### 3 | SCHUR COMPLEMENTS OF CLUSTERS AND GENERAL ESTIMATES

The condition number of  $\tilde{F}$  can be estimated in two steps. The first one is the subject of the following simple lemma.

**Lemma 1.** *Let there be constants  $0 < C_1 < C_2$  such that for each  $\lambda \in \mathbb{R}^m$*

$$C_1 \|\lambda\|^2 \leq \|\tilde{B}^T \lambda\|^2 \leq C_2 \|\lambda\|^2, \quad (7)$$

where  $\|\cdot\|$  denotes the Euclidean norm, and let  $\tilde{P}$  be defined by (6). Then

$$\bar{\kappa}(\tilde{P}\tilde{F}\tilde{P}) \leq \frac{C_2 \max\{\|\tilde{K}^i\| : i = 1, \dots, n_c\}}{C_1 \min\{\bar{\lambda}_{\min}(\tilde{K}^i) : i = 1, \dots, n_c\}}. \quad (8)$$

*Proof.* The proof of this lemma is rather trivial; it uses only the observations that if  $\lambda \in \text{Im}\tilde{P}$ , then  $\tilde{G}\lambda = \tilde{R}^T \tilde{B}^T \lambda = o$ , that is,  $\tilde{B}^T \lambda$  is orthogonal to the kernel of  $\tilde{K}$ , so that  $\tilde{B}^T \lambda \in \text{Im}\tilde{K}$ , that the nonzero eigenvalues of  $\tilde{K}$  are reciprocal to the corresponding eigenvalues of  $\tilde{K}^+$ , and that the spectrum  $\sigma(\tilde{K})$  of  $\tilde{K}$  satisfies

$$\sigma(\tilde{K}) = \bigcup_{i=1}^{n_c} \sigma(\tilde{K}^i).$$

The estimate given by Lemma 1 is a bit pessimistic. The reason is that  $\text{Im}\tilde{B}$  is spanned by the vectors that have zero components corresponding to the variables in the interior of  $\Omega^i$ . To enhance this observation, let us define the interface (skeleton)  $\Sigma$  of the decomposition by

$$\Sigma = \bigcup_{i=1}^{n_s} \Gamma^i \setminus \Gamma$$

and decompose the set of indices  $\mathcal{N}$  into the set of the indices of the skeleton nodes  $S$  and the interior nodes  $I$ . For any matrix  $A \in \mathbb{R}^{m \times n}$  and subsets  $\mathcal{I} \subseteq \{i = 1, \dots, m\}$  and  $\mathcal{J} \subseteq \{j = 1, \dots, n\}$ , let  $A_{\mathcal{I}, \mathcal{J}}$  denote a submatrix of  $A$  with the rows  $i \in \mathcal{I}$  and columns  $j \in \mathcal{J}$ . Then it is easy to check that

$$(\tilde{K}^+)_{SS} = \tilde{S}^+, \quad \tilde{S} = \tilde{K}_{SS} - \tilde{K}_{SI} \tilde{K}_{II}^{-1} \tilde{K}_{IS}.$$

The matrix  $\tilde{S}$  is called the Schur complement of  $S$  with respect to the block interior variables. The same formula holds for the clusters, that is,

$$((\tilde{K}^i)^+)_{S_i S_i} = (\tilde{S}^i)^+, \quad \tilde{S}^i = \tilde{K}_{S_i S_i}^i - \tilde{K}_{S_i I_i}^i (\tilde{K}_{I_i I_i}^i)^{-1} \tilde{K}_{I_i S_i}^i,$$

where  $S_i$  and  $I_i$  denote the skeleton and interior indices of the cluster, respectively. We can enhance these observations into the following corollary.

**Corollary 1.** *Let the assumptions of Lemma 1 be satisfied and let  $\tilde{P}$  be defined by (6). Then*

$$\overline{\kappa}(\tilde{P} \tilde{F} \tilde{P}) \leq \frac{C_2 \max\{\|\tilde{S}^i\| : i = 1, \dots, n_c\}}{C_1 \min\{\bar{\lambda}_{\min}(\tilde{S}^i) : i = 1, \dots, n_c\}}. \quad (9)$$

The regular condition number of  $S^i$  is known to be bounded by  $CH/h$ , see, for example, Pechstein [22, lemma 1.59].

## 4 | JOINING SQUARE SUBDOMAINS BY AVERAGES

In what follows, we shall denote by  $e$  and  $\bar{e}$  the vectors with all components equal to 1 and  $1/\|e\|$ , respectively, where  $\|\cdot\|$  denotes the Euclidean norm. To simplify the notations, we shall often avoid specification of the dimension of vectors and matrices when it can be deduced from the assumption that they appear in well-defined expressions or when we introduce a generic object as above. It is thus possible that one symbol can represent in one formula two objects of different dimensions.

To describe the joining by averages, we shall use the transformation of bases proposed by Klawonn and Widlund,<sup>20</sup> see also Klawonn and Rheinbach<sup>23</sup> and Li and Widlund.<sup>24</sup> The basic idea is a rather trivial observation that

$$x^T e = \sum_{i=1}^p x_i,$$

so if

$$[c_1, \dots, c_{p-1}, \bar{e}], \quad \bar{e} = \frac{1}{\sqrt{p}} e,$$

denote an orthonormal basis of  $\mathbb{R}^p$ , then the last coordinate of a vector  $x \in \mathbb{R}^p$  in this basis is given by  $x_p = \bar{e}^T x$ .

To find the basis and transformation, denote by  $T \in \mathbb{R}^{p \times p}$  an orthogonal matrix that can be obtained by the application of the Gram–Schmidt procedure to the columns of

$$T_0 = \begin{bmatrix} I & e \\ -e^T & 1 \end{bmatrix} \in \mathbb{R}^{p \times p},$$

starting from the last one. We get

$$T = [C, \bar{e}], \quad C^T C = I, \quad C^T \bar{e} = o, \quad \|\bar{e}\| = 1, \quad C \in \mathbb{R}^{p \times (p-1)}, \quad \bar{e} \in \mathbb{R}^p, \quad (10)$$

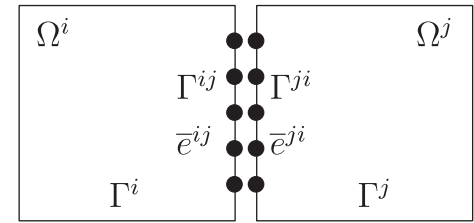
and if  $x = Ty$ ,  $y \in \mathbb{R}^p$ , then

$$y_p = \bar{e}^T x = \frac{1}{\sqrt{p}} \sum_{i=1}^p x_i, \quad \bar{e} = \frac{1}{\sqrt{p}} e.$$

If we apply the transformation to variables associated with the interiors of adjacent edges, we can join them by the extension mapping  $L$  as above. Let us first show how to join two subdomains  $\Omega^1$  and  $\Omega^2$  by the averages of variables associated with the interior of adjacent edges. The basis normalized constant vectors associated with interior of the edge  $\Gamma^{ij}$  of  $\Omega^i$  adjacent to  $\Omega^j$  will be denoted by  $\bar{e}^{ij}$  as in Figure 4,  $\bar{e}^{ij} \in \mathbb{R}^{n_e}$ .

On the interiors of edges  $\Gamma^{12}$  and  $\Gamma^{21}$ , we shall introduce the transformation matrices  $T^{12}, T^{21} \in \mathbb{R}^{n_e \times n_e}$ ,

$$x^{12} = T^{12} y^{12}, \quad x^{21} = T^{21} y^{21}, \quad T^{ij} = [C^{ij}, \bar{e}^{ij}] \in \mathbb{R}^{n_e \times n_e}, \quad (T^{ij})^T T^{ij} = I,$$

**FIGURE 4** Joining two subdomains by the edge averages

so that we can define orthogonal transformations  $T^1, T^2 \in \mathbb{R}^{n_s \times n_s}$ , acting on the boundaries of  $\Omega^1$  and  $\Omega^2$  by

$$T^1 = \begin{bmatrix} I & O \\ O & T^{12} \end{bmatrix} = \begin{bmatrix} I & O & o \\ O & C^{12} & \bar{e}^{12} \end{bmatrix}, \quad T^2 = \begin{bmatrix} I & O \\ O & T^{21} \end{bmatrix} = \begin{bmatrix} I & O & o \\ O & C^{21} & \bar{e}^{21} \end{bmatrix}.$$

The identity matrix is associated with the variables that are not affected by joining. The global transformation  $T \in \mathbb{R}^{n \times n}$ ,  $n = 2n_s$ , then reads

$$T = \begin{bmatrix} T^1 & O \\ O & T^2 \end{bmatrix} = \begin{bmatrix} I & O & O & O \\ O & T^{12} & O & O \\ O & O & I & O \\ O & O & O & T^{21} \end{bmatrix} = \begin{bmatrix} I & O & o & O & O & o \\ O & C^{12} & \bar{e}^{12} & O & O & o \\ O & O & o & I & O & o \\ O & O & o & O & C^{21} & \bar{e}^{21} \end{bmatrix}.$$

Since we are especially interested in the columns corresponding to averages, it is convenient to move the columns with  $\bar{e}^{ij}$  to the right to get

$$T_{\Pi} = \begin{bmatrix} I & O & O & O & o & o \\ O & C^{12} & O & O & \bar{e}^{12} & o \\ O & O & I & O & o & o \\ O & O & O & C^{21} & o & \bar{e}^{21} \end{bmatrix} = \begin{bmatrix} C^1 & O & \bar{e}^{12} & o \\ O & C^2 & o & \bar{e}^{21} \end{bmatrix} \in \mathbb{R}^{n \times n}.$$

The joining can then be implemented by the normalized expansion matrix

$$L = \begin{bmatrix} I & O & o \\ O & I & o \\ o^T & o^T & 1/\sqrt{2} \\ o^T & o^T & 1/\sqrt{2} \end{bmatrix} = \begin{bmatrix} I & o \\ o^T & 1/\sqrt{2} \\ o^T & 1/\sqrt{2} \end{bmatrix} \in \mathbb{R}^{n \times (n-1)}.$$

Using  $T_{\Pi}$  and  $L$ , we can define

$$Z = T_{\Pi}L = \begin{bmatrix} I & O & O & O & o \\ O & C^{12} & O & O & 1/\sqrt{2}\bar{e}^{12} \\ O & O & I & O & o \\ O & O & O & C^{21} & 1/\sqrt{2}\bar{e}^{21} \end{bmatrix} = \begin{bmatrix} C^1 & O & 1/\sqrt{2}\bar{e}^{12} \\ O & C^2 & 1/\sqrt{2}\bar{e}^{21} \end{bmatrix} = [C \ E],$$

$Z \in \mathbb{R}^{n \times (n-1)}$ ,  $C \in \mathbb{R}^{n \times (n-2)}$ ,  $E \in \mathbb{R}^n$ , the columns of which span the subspace of feasible vectors. Indeed, using (10) and the definition of  $T_{\Pi}$ , we can check that the interior edge variables  $x^{12}$  and  $x^{21}$  of any vector  $x = Zy$ ,

$$x = \begin{bmatrix} x^1 \\ x^{12} \\ x^2 \\ x^{21} \end{bmatrix} = \begin{bmatrix} I & O & O & O & o \\ O & C^{12} & O & O & 1/\sqrt{2}\bar{e}^{12} \\ O & O & I & O & o \\ O & O & O & C^{21} & 1/\sqrt{2}\bar{e}^{21} \end{bmatrix} \begin{bmatrix} y^1 \\ y^{12} \\ y^2 \\ y^{21} \\ y_{n-1} \end{bmatrix},$$

satisfy (with  $\bar{e} \in \mathbb{R}^{n_e}$ ,  $\bar{e}^T \bar{e} = 1$ )

$$\begin{aligned}\bar{e}^T x^{12} &= \bar{e}^T (C^{12} y^{12} + 1/\sqrt{2} y_{n-1} \bar{e}^{12}) = 1/\sqrt{2} y_{n-1}, \\ \bar{e}^T x^{21} &= \bar{e}^T (C^{21} y^{21} + 1/\sqrt{2} y_{n-1} \bar{e}^{21}) = 1/\sqrt{2} y_{n-1}.\end{aligned}$$

Recall that  $\bar{e}^{ij} \in \mathbb{R}^{n_e}$  denotes a vector with  $n_e$  entries equal  $1/\sqrt{n_e}$  associated with the interior of part of  $\Gamma^{ij}$  and  $C^{ij} \in \mathbb{R}^{n_e \times (n_e-1)}$ . Notice that the feasible vectors can be described in a much simpler way using

$$\text{Im}Z = \{x \in \mathbb{R}^n : x^T Z_\perp = 0\} = (\text{Im}Z_\perp)^\perp, \quad Z_\perp = \begin{bmatrix} 1/\sqrt{2} \bar{e}^{12} \\ -1/\sqrt{2} \bar{e}^{21} \end{bmatrix}.$$

The procedure can be generalized to specify the feasible vectors of any cluster joined by the averages of any set of adjacent edges. Here, we shall consider the clusters formed by  $m^2$  square subdomains ordered as in Figure 1 and joined by some edge averages. Using proper numbering of variables by subdomains, in each subdomain setting first the variables that are not affected by joining, then the variables associated with the averages ordered by edges, we get

$$Z = \begin{bmatrix} C & E \end{bmatrix}, \quad C = \text{diag}(C^1, \dots, C^s), \quad E = 1/\sqrt{2} \begin{bmatrix} \cdot & \cdot & \cdot \\ \cdot & \bar{e}^{ij} & \cdot \\ \cdot & \cdot & \cdot \\ \cdot & -\bar{e}^{ji} & \cdot \\ \cdot & \cdot & \cdot \end{bmatrix}, \quad (i, j) \in \mathcal{C},$$

where  $\mathcal{C}$  denotes the set of ordered couples of indices that define joining of adjacent edges by averages. It is not necessary that  $(i, j) \in \mathcal{C}$  whenever  $\Omega^i$  has an adjacent edge with  $\Omega^j$ . To avoid duplicity, we assume that  $(i, j) \in \mathcal{C}$  implies  $i < j$ . Each column of  $E$  corresponds to an interface between some subdomains  $\Omega^i$  and  $\Omega^j$  and comprises two nonzero block entries of the dimensions corresponding to the number of columns of the matrices  $C^i$  and  $C^j$ , each of which has just  $n_e$  nonzero entries equal to  $1/\sqrt{n_e}$ .

The columns of  $Z$  form an orthonormal basis of the subspace of feasible vectors. As above, we can form the matrix  $Z_\perp$  from the last block of  $E$  by changing the sign of one of the two nonzero block components in each column. Notice that both  $Z$  and  $Z_\perp$  have orthonormal columns and that  $U = [Z, Z_\perp]$  is an orthogonal matrix.

## 5 | BOUNDS ON THE SPECTRUM OF CHAIN CLUSTERS

Let us denote

$$S = \text{diag}(S^1, \dots, S^s) \quad \text{and} \quad \tilde{S} = Z^T S Z.$$

While the dimension of the kernel of  $S$  is  $s$ , the kernel of  $\tilde{S}$  is spanned by a unique vector

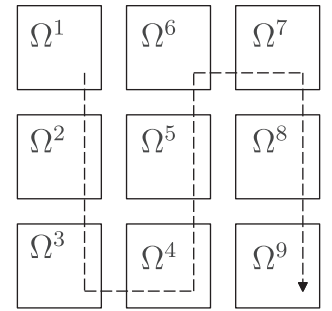
$$\tilde{r} = Z^T \bar{r}, \quad \bar{r} = \frac{1}{\sqrt{n_c}} [1, \dots, 1]^T \in \mathbb{R}^{n_c}, \quad n_c = s n_s.$$

Since  $Z^T Z = I$ , it is rather trivial to see that the upper bound on the spectrum of  $\tilde{S}$  is given by

$$\lambda_{\max}(\tilde{S}) \leq \max_i \|S^i\|, \quad i = 1, \dots, s.$$

To get a lower bound on the nonzero eigenvalues of  $\tilde{S}$ , notice that

$$\min_{\zeta \in \text{Im} \tilde{S}} \zeta^T \tilde{S} \zeta = \min_{\zeta^T \bar{r} = 0} \zeta^T Z^T S Z \zeta \geq \bar{\lambda}_{\min}(S) \min_{\zeta^T \bar{r} = 0} \|P_{\text{Im} s} Z \zeta\|^2, \quad (11)$$

**FIGURE 5** The chain of the subdomains

and denote by  $R$  and  $R_{\perp}$  the matrices with orthonormal columns such that

$$\text{Im } R = \text{Ker } S, \quad R \in \mathbb{R}^{n_c \times s}, \quad \text{Im } R_{\perp} = \text{Im } S, \quad R_{\perp} \in \mathbb{R}^{n_c \times (n_c - s)}.$$

It follows that  $[R_{\perp}, R]$  is orthogonal,  $P_{\text{Im } S} = R_{\perp} R_{\perp}^T$  is an orthogonal projector on  $\text{Im } S$ , and

$$\min_{\zeta^T \tilde{r}=0} \|P_{\text{Im } S} Z \zeta\|^2 = \min_{\zeta^T \tilde{r}=0} \|R_{\perp}^T Z \zeta\|^2. \quad (12)$$

The relations (11) and (12) are valid for any coupling set  $C$ . In this section, we consider the coupling set denoted by

$$C_{\text{chain}} = (1, 2), (2, 3), \dots, (m^2 - m, m^2), \quad s = m^2.$$

Notice that the square subdomains of Figure 1 can be joined by the edge averages into a chain as in Figure 5.

Examining the structure of  $Z$ , we can check that if  $C_{\text{chain}} \subseteq C$ , then

$$\text{Im } Z \cap \text{Im } R = \text{span}(e_c), \quad \text{Im } Z_{\text{chain}} \supseteq \text{Im } Z, \quad \text{and} \quad e_c = [1, \dots, 1]^T \in \mathbb{R}^{n_c}, \quad (13)$$

where  $Z_{\text{chain}}$  denotes an instance of  $Z$  associated with  $C_{\text{chain}}$ . It follows that

$$\min_{\zeta^T \tilde{r}=0} \|R_{\perp}^T Z \zeta\|^2 \geq \min_{\zeta^T \tilde{r}=0} \|R_{\perp}^T Z_{\text{chain}} \zeta\|^2, \quad (14)$$

and combining (11), (12), and (14), we get

$$\min_{\zeta \in \text{Im } \tilde{S}} \zeta^T \tilde{S} \zeta \geq \bar{\lambda}_{\min}(S) \min_{\zeta^T \tilde{r}=0} \|R_{\perp}^T Z_{\text{chain}} \zeta\|^2. \quad (15)$$

To estimate the right-hand side of (14), let us simplify the notation by denoting  $Z = Z_{\text{chain}}$  till the end of this section and recall that the matrices  $[Z, Z_{\perp}]$  and  $[R_{\perp}, R]$  are orthogonal as well as

$$W = \begin{bmatrix} R_{\perp}^T \\ R^T \end{bmatrix} [Z \quad Z_{\perp}] = \begin{bmatrix} R_{\perp}^T Z & R_{\perp}^T Z_{\perp} \\ R^T Z & R^T Z_{\perp} \end{bmatrix}.$$

Using the CS decomposition (see, e.g., Stewart [25, section 4.5]), we get that there are orthogonal matrices  $U = \text{diag}(U_1, U_2)$  and  $V = \text{diag}(V_1, V_2)$  such that

$$U^T Z V = \begin{bmatrix} U_1 R_{\perp}^T Z V_1 & U_1 R_{\perp}^T Z_{\perp} V_2 \\ U_2 R^T Z V_1 & U_2 R^T Z_{\perp} V_2 \end{bmatrix} = \left[ \begin{array}{cc|cc} I & & O & \\ & C & & S \\ \hline & & O & I \\ O & & I & \\ \hline & & -S & C \\ & & & O \\ & & I & \end{array} \right], \quad (16)$$

where  $C = \text{diag}(c_1, \dots, c_k)$ ,  $c_i \in (0, 1)$ ,  $S = \text{diag}(s_1, \dots, s_k)$ , and  $C^2 + S^2 = I$ . Some of the matrices  $I, C, O$  can be missing, the exact rule can be derived from the fact that the global matrix has orthonormal rows and columns. The blocks  $O$  can be rectangular and can have different size.

Notice that the CS decomposition (16) provides the singular value decomposition of four blocks by means of only four orthogonal matrices. Comparing the diagonal blocks of the last two matrices in (16), we get that the set of singular values of  $R_{\perp}^T Z$  and  $R^T Z_{\perp}$  in the interval  $(0, 1)$  are identical—see also Ipsen and Mayer.<sup>26</sup>

To evaluate explicitly the smallest singular value  $\bar{\sigma}_{\min}$  of  $R^T Z_{\perp}$ , notice that

$$Z_{\perp} = \sqrt{\frac{1}{2}} \begin{bmatrix} e^{12} & 0 & \dots & 0 & 0 \\ -e^{21} & e^{23} & \ddots & 0 & 0 \\ 0 & -e^{32} & \ddots & 0 & 0 \\ \vdots & \ddots & \ddots & \ddots & \vdots \\ 0 & 0 & \ddots & -e^{s-1,s-2} & e^{s-1,s} \\ 0 & 0 & \dots & 0 & -e^{s,s-1} \end{bmatrix},$$

and recall that  $R = \text{diag}(r^1, \dots, r^s)$ ,  $e^{ij} \in \mathbb{R}^{n_s}$ ,  $\|r^i\| = \|e^{ij}\| = 1$ . Since  $e^{ij}$  have  $n_e$  nonzero entries equal to  $1/\sqrt{n_e}$ , we get

$$(r^i)^T e^{i,i+1} = -(r^{i+1})^T e^{i+1,i} = \frac{n_e}{\sqrt{n_e} \sqrt{n_s}} = \sqrt{\frac{n_e}{n_s}}, \quad i = 1, \dots, s-1,$$

$$R^T Z_{\perp} = \sqrt{\frac{n_e}{2n_s}} \begin{bmatrix} 1 & 0 & 0 & \dots & 0 & 0 \\ -1 & 1 & 0 & \dots & 0 & 0 \\ \vdots & \ddots & \ddots & \dots & \ddots & \ddots \\ 0 & 0 & 0 & \dots & -1 & 1 \\ 0 & 0 & 0 & \dots & 0 & -1 \end{bmatrix} = \sqrt{\frac{n_e}{2n_s}} B \in \mathbb{R}^{s \times (s-1)}, \quad (17)$$

and

$$(R^T Z_{\perp})^T R^T Z_{\perp} = \frac{n_e}{2n_s} \begin{bmatrix} 2 & -1 & 0 & \dots & 0 & 0 \\ -1 & 2 & -1 & \dots & 0 & 0 \\ \vdots & \ddots & \ddots & \dots & \ddots & \ddots \\ 0 & 0 & 0 & \dots & 2 & -1 \\ 0 & 0 & 0 & \dots & -1 & 2 \end{bmatrix} \in \mathbb{R}^{(s-1) \times (s-1)}.$$

Notice that  $B = [b_{ij}]$  has all its entries equal to zero except  $b_{ii} = 1$  and  $b_{ji} = -1$  for  $(i, j) \in C$ .

We can easily recognize that the matrix in the above formula is the discrete Laplacian. Its eigenvalues are well known [27, excercise 7.2.18], in particular the smallest eigenvalue is given by

$$\lambda_1 = \sigma_{\min}^2(R^T Z_{\perp}) = 4 \sin^2\left(\frac{\pi}{2s}\right).$$

It follows that

$$R^T Z_{\perp} \in \mathbb{R}^{s \times (s-a)}$$

is a full rank matrix. Replacing  $R^T Z_{\perp}$  by its SVD decomposition

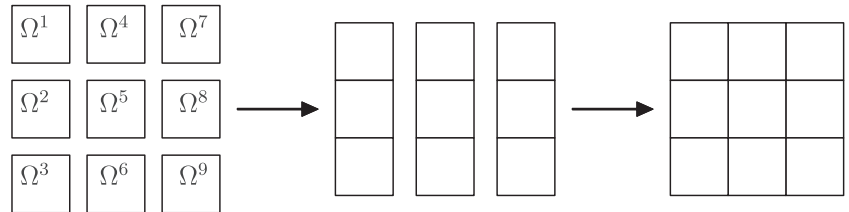
$$R^T Z_{\perp} = U \Sigma V^T, \quad \Sigma = \text{diag}(\sigma_1, \dots, \sigma_{s-1}) \in \mathbb{R}^{s \times (s-1)}, \quad \sigma_1 \geq \dots \geq \sigma_{s-1} = \bar{\sigma}_{\min} > 0,$$

we get

$$\min_{\zeta \in \text{Im } S} \zeta^T \tilde{S} \zeta \geq \bar{\lambda}_{\min}(S) \min_{\zeta^T \tilde{r} = 0} \|U \Sigma V^T \zeta\|^2 = \bar{\lambda}_{\min}(S) \bar{\sigma}_{\min}^2 \|\zeta\|^2. \quad (18)$$

Combining the above reasoning with Corollary 1, we can state the following theorem.

**FIGURE 6** Interconnecting subdomains into chains and joining chains into a square cluster



**Theorem 1.** Let  $\tilde{S}$  denote the Schur complement of a chain cluster comprising  $s$  square subdomains of  $\Omega$  with the edge-length  $H_s = 1/m$  and discretized by the regular grid with the steplength  $h$ . Let  $\bar{\lambda}_{\min}(S)$  denote the smallest nonzero eigenvalue of the Schur complements  $S$  of the subdomain. Then

$$\bar{\lambda}_{\min}(S) \geq \bar{\lambda}_{\min}(\tilde{S}) \geq \frac{2n_e}{n_s} \bar{\lambda}_{\min}(S) \sin^2\left(\frac{\pi}{2s}\right) \approx \frac{1}{2} \bar{\lambda}_{\min}(S) \left(\frac{\pi}{2s}\right)^2 \quad (19)$$

and there is a constant  $C$  such that for any  $h$ ,  $H_s$ , and  $s$

$$\bar{\kappa}(\tilde{S}) \leq C \frac{H_s s^2}{h}. \quad (20)$$

## 6 | BOUNDS ON THE SPECTRUM OF SQUARE CLUSTERS

Equation (20) gives an upper bound on  $\bar{\kappa}(\tilde{S})$  for quite general clusters, but it is rather pessimistic for more compact ones. Here, we shall prove that for the square clusters joined by the edge averages, it is possible to replace  $s^2$  in (20) by  $s = m^2$ .

Let us consider a cluster formed by  $m \times m$  square  $H_s \times H_s$  subdomains that are joined by the edge averages of the variables associated with the interiors of adjacent edges. Using the procedure described above, we shall reduce the problem to the analysis of singular values of the matrix  $R^T Z_\perp$ , which is now a bit more complicated, but still nicely structured. Let us start with the  $3 \times 3$  cluster comprising nine subdomains numbered as in Figure 1 joined by the edge averages along all 12 interfaces. The interconnecting can be represented by the matrix

$$R^T Z_\perp = \sqrt{\frac{n_e}{2n_s}} \begin{bmatrix} B & O & O & I & O \\ O & B & O & -I & I \\ O & O & B & O & -I \end{bmatrix}, \quad (21)$$

where the matrix  $B$  given by

$$B = \begin{bmatrix} 1 & 0 \\ -1 & 1 \\ 0 & -1 \end{bmatrix}$$

corresponds to the joining of subdomains into vertical chains and the last two columns correspond to joining vertical chains to the square cluster as in Figure 6.

The matrix (21) can be conveniently analyzed by means of Kronecker product. Recall that if  $A = a_{ij} \in \mathbb{R}^{m \times n}$  and  $C \in \mathbb{R}^{p \times q}$  are given matrices, then their Kronecker product  $A \otimes C$  is defined by

$$A \otimes C = \begin{bmatrix} a_{11}C & \dots & a_{1n}C \\ \vdots & \vdots & \vdots \\ a_{m1}C & \dots & a_{mn}C \end{bmatrix} \in \mathbb{R}^{mp \times nq}.$$

Relevant Kronecker product properties include

$$(\alpha A) \otimes C = A \otimes (\alpha C) = \alpha(A \otimes C), \quad (22)$$

$$(A \otimes C)^T = A^T \otimes C^T, \quad (23)$$

$$(A \otimes C)(D \otimes E) = (AD \otimes CE). \quad (24)$$

The dimensions of the matrices in (24) must comply with the definitions of  $AD$  and  $CE$  so that the latter products exist. The properties (22)–(24) can be verified directly by computations. See also the books by Golub and Van Loan [28, chapter 12] or Horn and Johnson [29, chapter 6].

Let us now rewrite (21) by means of the Kronecker product to get

$$R^T Z_{\perp} = \sqrt{\frac{n_e}{2n_s}} [I \otimes B, B \otimes I] \quad (25)$$

and use (23) and (24) to obtain

$$R^T Z_{\perp} (R_{\perp}^T)^T = \frac{n_e}{2n_s} (I \otimes BB^T + BB^T \otimes I). \quad (26)$$

The latter is the Kronecker sum, the eigenvalues of which can be expressed by the eigenvalues  $\lambda_i$  of  $BB^T$  (see, e.g., References 29 or 30). Denoting by  $\sigma(A)$  the spectrum of a given square matrix  $A$ , we have

$$\sigma(I \otimes BB^T + BB^T \otimes I) = \{\lambda_i + \lambda_j : \lambda_i, \lambda_j \in \sigma(BB^T)\}.$$

Since zero is obviously a simple eigenvalue of  $BB^T$ , we conclude that

$$\bar{\sigma}_{\min}^2(R^T Z_{\perp}) = \bar{\lambda}_{\min}(R^T Z_{\perp} (R_{\perp}^T)^T) \geq \frac{n_e}{2n_s} \bar{\lambda}_{\min}(BB^T) = \frac{n_e}{2n_s} \bar{\lambda}_{\min}(B^T B). \quad (27)$$

The arguments presented above are obviously valid for any  $m$ . We have thus managed to reduce the estimate to that related to the short chain of the length  $m$ . We can thus formulate the main result of this section.

**Theorem 2.** *For each integer  $m > 1$ , let  $\tilde{S}$  denote the Schur complement of the  $m \times m$  cluster with the side-length  $H_c$  comprising  $s = m^2$  square subdomains of the side-length  $H_s = H_c/m$  discretized by the regular grid with the step-length  $h$ . Let  $\bar{\lambda}_{\min}(S)$  denote the smallest nonzero eigenvalue of the Schur complement  $S$  of the subdomain matrices  $K^i$ ,  $i = 1, \dots, s$  with respect to the interior variables. Then*

$$\|S\| = \lambda_{\max}(S) \geq \lambda_{\max}(\tilde{S}), \quad (28)$$

$$\bar{\lambda}_{\min}(S) \geq \bar{\lambda}_{\min}(\tilde{S}) \geq \frac{2n_e}{n_s} \bar{\lambda}_{\min}(S) \sin^2\left(\frac{\pi}{2m}\right) \approx \frac{1}{2} \bar{\lambda}_{\min}(S) \left(\frac{\pi}{2m}\right)^2, \quad (29)$$

and there is a constant  $C$  such that for any  $h$ ,  $H_s$ , and  $m$

$$\bar{\kappa}(\tilde{S}) \leq C \frac{H_s m^2}{h}. \quad (30)$$

*Proof.* The inequalities (28) and (29) were proved above. To get (30), notice that by (28) and (29)

$$\bar{\kappa}(\tilde{S}) \leq \bar{\kappa}(S) \frac{n_s}{2n_e} \sin^{-2}\left(\frac{\pi}{2m}\right) \leq C \bar{\kappa}(S) m^2. \quad \blacksquare$$

To complete our analysis, we can combine Corollary 1 with Theorem 2 to get a bound on the conditioning of H-TFETI-DP dual stiffness matrix  $\tilde{F}$  for joining of square subdomains into square clusters by the edge averages.

**Corollary 2.** *Let the domain  $\Omega$  be decomposed and discretized by a uniform grid with parameters  $H_c$  and  $h$ , respectively, let each subdomain be decomposed into  $m \times m$  square subdomains with the edge-length  $H_s = H_c/m$  joined by the edge averages. Then there is a constant  $C$  such that for any  $h$ ,  $H_c$ , and  $m$*

$$\bar{\kappa}(\tilde{F}) \leq C m \frac{H_c}{h}. \quad (31)$$

**TABLE 1** Regular condition number and extreme nonzero eigenvalues

<b>m=</b>	<b>2</b>	<b>4</b>	<b>8</b>	<b>16</b>
$H_s/h$	32	16	8	4
$\bar{\lambda}_{\max}(\tilde{S})$	2.8235	2.8098	2.7638	2.6843
$\bar{\lambda}_{\min}(\tilde{S})$	0.0173	0.0093	0.0047	0.0022
$\bar{\lambda}_{\min}^{\text{est}}(\tilde{S})$	0.0104	0.0059	0.0029	0.0012
$\bar{\lambda}_{\min}(S)$	0.0430	0.0859	0.1712	0.3372
$\kappa(\tilde{S})$	163.2081	302.1290	588.0426	1220.1363

Corollary 2 is sufficient to extend the scalability of FETI-based algorithms for model problem (1) to H-TFETI-DP. If there are no Signorini conditions, then the dual problem reduces to the solution of

$$\tilde{P}\tilde{F}\tilde{P}\lambda = \tilde{P}\tilde{d}, \quad \tilde{P} = I - \tilde{G}^T(GG^T)^{-1}\tilde{G},$$

where  $\tilde{G}$ ,  $\tilde{P}$ ,  $\tilde{F}$  are from (5). The latter problem can be solved by a uniformly bounded number of conjugate gradient iterations provided  $m$ ,  $h$ , and  $H_c$  satisfy

$$mH_c/h \leq C$$

for a sufficiently large positive constant  $C > 0$ . If there are Signorini conditions, then the same result can be obtained for the solution of the dual problem (5) if we replace the subdomains by clusters in the scalable TFETI algorithms described in Reference 21. See also Reference [4, chapter 10].

## 7 | NUMERICAL EXPERIMENTS

We carried out some numerical experiments to check how tight the bound is and to compare the performance of TFETI, a well-established computational engine of scalable algorithms for elliptic variational equalities and inequalities, see, for example, 21 or [4, chapter 10], with H-TFETI.

### 7.1 | Comparing estimate and experiments

To compare our estimate with the specific values, we computed the bounds on nonzero eigenvalues and the extreme eigenvalues of the Schur complements of  $m \times m$  clusters with  $H_c = 1$ ,  $H_s = 1/m$ , and  $h = 1/64$ ,  $m \in \{2, 4, 8, 16\}$ . We considered clusters obtained by joining edge averages. The results are in Table 1.

The results show that the bounds provide realistic lower bounds on the extreme eigenvalues of  $\tilde{S}$  and comply with both our theoretical results and the experimental results by Klawonn and Rheinbach<sup>6</sup> and Lee and Widlund<sup>12</sup> (they call the method FETI-FETI). The results confirm promising results for the clusters joined by averages. Notice that the condition number increases proportionally to  $m$  as predicted by the theory, but the rank of the projector to the natural coarse grid and the degree of parallelization decreases proportionally with  $m^4$ .

### 7.2 | Comparing unpreconditioned H-TFETI-DP and TFETI

In this section, the performance of H-TFETI-DP was compared with the standard TFETI approach on the unit square Poisson benchmark discretized by Q1 finite elements. Both algorithms were implemented in the exascale parallel FETI solver package<sup>31</sup> developed at IT4Innovations, Czech National Supercomputing Center. Computations were performed on the Salomon cluster which consists of 1008 compute nodes. Each node contains 24 core Intel Xeon E5-2680v3 processors with 128 GB RAM, interconnected by 7D Enhanced hypercube InfiniBand.

The domain was decomposed into  $n_c \times n_c$  clusters,  $n_c = 6, 12, 18, 36, 54$ , each cluster comprising  $15 \times 15$  square subdomains  $H_s \times H_s$  joined by edge averages and discretized by the regular grid with the discretization parameter  $h$ ,  $H_s/h = 100$ . The number of subdomains and unknowns ranged from 8000 to 656,000 and from 81,018,001 to 6,561,162,001, respectively (see Table 2). Stopping criteria of the relative residual in the projected conjugate gradient method was set to  $\varepsilon = 1 \cdot 10^{-4}$ .

Clusters	Subdomains	Unknowns	iter/time (s)	iter/time (s)
			H-TFETI-DP	TFETI
36	8100	81,018,001	117/26.0	45/14.5
144	32,400	324,036,001	127/29.1	44/23.7
324	72,900	729,054,001	118/27.7	42/40.2
1296	291,600	2,916,108,001	117/28.0	41/45.0
2916	656,100	6,561,162,001	116/28.0	41/61.0

**TABLE 2** Billion Poisson equation—unpreconditioned H-TFETI and TFETI,  $m = 15$

We can see that the iterations of the H-TFETI-DP algorithm without preconditioning are bounded as in the TFETI algorithm, but the number of iterations is approximately 2.8 times higher for the H-TFETI-DP algorithm, which approximately agrees with  $\sqrt{15}$  predicted by the well-known estimate of the rate of convergence of the conjugate gradient methods. Most important, the computational time is almost constant for the H-TFETI algorithm, unlike TFETI, because of a bottleneck in the solution of TFETI coarse problems for a larger number of domains. For the largest problem in Table 2, H-TFETI-DP was more than twice faster than TFETI.

## 8 | COMMENTS AND CONCLUSIONS

We have established bounds on the regular condition number of the Schur complements of floating clusters arising from the interconnecting of square subdomains by edge averages. The estimates were confirmed by numerical experiments and plugged into the analysis of unpreconditioned H-TFETI-DP algorithms. In particular, the results show that joining the subdomains into  $m \times m$  clusters increases  $\sqrt{m}$ -times the number of iterations that are necessary to achieve a prescribed relative precision and reduces  $m^4$ -times the cost of preparation of the coarse problem. Both the theoretical results and numerical experiments indicate, rather surprisingly, that unpreconditioned H-TFETI-DP with large clusters can be a competitive computational engine for the solution of huge systems of linear equations discretized by sufficiently structured regular grids. Using the reorthogonalization-based preconditioning,<sup>32</sup> the same performance can be achieved for the problems with variable coefficients provided they are constant on the clusters. The methods of proofs can be used to get some results for more general grids, particularly those obtained by the deformation of a structured grid and for 3D problems.

The results presented can be useful for extending the scope of scalability of the FETI-based algorithms for the solution of variational inequalities. While the TFETI algorithms have already proved to be effective for the solution of variational inequalities discretized by billions of nodal variables using tens of thousands cores,<sup>4</sup> the results presented here suggest that H-TFETI-DP can solve at least ten-times larger problems using hundreds of thousands cores. Further improvements can be achieved by joining the corners and modifications proposed for H-FETI-DP.<sup>7</sup>

## ACKNOWLEDGMENTS

This work was supported by The Ministry of Education, Youth and Sports from the National Programme of Sustainability (NPS II) project IT4Innovations excellence in science: LQ1602 and by the IT4Innovations infrastructure which is supported from the Large Infrastructures for Research, Experimental Development and Innovations project IT4Innovations National Supercomputing Center: LM2015070.

## ORCID

Zdeněk Dostál  <https://orcid.org/0000-0002-3252-4795>

## REFERENCES

1. Farhat C, Roux F-X. A method of finite element tearing and interconnecting and its parallel solution algorithm. *Int J Numer Methods Eng.* 1991;32:1205–1227.
2. Farhat C, Roux F-X. An unconventional domain decomposition method for an efficient parallel solution of large-scale finite element systems. *SIAM J Sci Comput.* 1992;13:379–396.
3. Farhat C, Mandel J, Roux F-X. Optimal convergence properties of the FETI domain decomposition method. *Comput Methods Appl Mech Eng.* 1994;115:365–385.

4. Dostál Z, Kozubek T, Sadowská M, Vondrák V. Scalable algorithms for contact problems, AMM 36. New York, NY: Springer, 2016.
5. Toselli A, Widlund OB. Domain decomposition methods – algorithms and theory. Springer series on computational mathematics. Vol 34. Berlin, Germany: Springer, 2005.
6. Klawonn A, Rheinbach O. A hybrid approach to 3-level FETI. Proc Appl Math Mech. 2010;90(1):5–32.
7. Klawonn A, Rheinbach O. Highly scalable parallel domain decomposition methods with an application to biomechanics. Z Angew Math Mech. 2010;90(1):5–32.
8. Klawonn A, Langer M, Rheinbach O. Toward extremely scalable nonlinear domain decomposition methods for elliptic partial differential equations, SIAM. J Sci Comput. 2015;37(1):C667–C696.
9. Farhat C, Lesoinne M, Pierson K. A scalable dual-primal domain decomposition method. Numer Lin Algebra and Appl. 2000;7(7–8):687–714.
10. Brzobohatý T, Jarošová M, Kozubek T, Menšík M, Markopoulos A. The hybrid total FETI method. Proceedings of the 3rd International Conference on Parallel, Distributed, Grid, and Cloud Computing for Engineering Civil-Comp; Stirlingshire; 2013.
11. Markopoulos A, Říha L, Brzobohatý T, Meca O, Kučera R, Kozubek T. The HTFETI method variant gluing cluster subdomains by kernel matrix representing the rigid body motions. In: Bjørstad PE, Brenner SC, Helpert L, Kim HH, Kornhuber R, Rahman T & Widlund OB et al., editors. Proceedings of DDM24 LNCSE 125. Cham: Springer, 2018.
12. Lee J. Domain decomposition methods for auxiliary linear problems of an elliptic variational inequality. In: Bank R, Holst M, Widlund O & Xu J et al., editors. Domain decomposition methods in science and engineering XX, lecture notes in computational science and engineering. Volume 91, 2013; p. 319–326. Heidelberg: Springer.
13. Lee J. Two domain decomposition methods for auxiliary linear problems for a multibody variational inequality. SIAM J Sci Comput. 2013;35(3):1350–1375.
14. Dostál Z, Horák D, Kučera R. Total FETI - an easier implementable variant of the FETI method for numerical solution of elliptic PDE. Commun Numer Methods Eng. 2006;22:1155–1162.
15. Dostál Z. Optimal quadratic programming algorithms, with applications to variational inequalities. 1st ed. New York, NY: Springer, 2009.
16. Vodstrčil P, Bouchala J, Jarošová M, Dostál Z. On conditioning of Schur complements of H-TFETI clusters for 2D problems governed by Laplacian. Appl Math. 2017;62(6):699–718.
17. Schöberl J. Solving the Signorini problem on the basis of domain decomposition techniques. Computing. 1998;60:323–344.
18. Dostál Z, Gomes FAM, Santos SA. Duality based domain decomposition with natural coarse space for variational inequalities. J Comput Appl Math. 2000;126(1–2):397–415.
19. Farhat C, Lesoinne M, LeTallec P, Pierson K, Rixen D. A dual-primal unified FETI method I – a faster alternative to the two-level FETI method. Int J Numer Methods Eng. 2001;50(7):1524–1544.
20. Klawonn A, Widlund O. Dual-primal FETI method for linear elasticity. Commun Pure Appl Math J Issued Courant Inst Math Sci. 2006;59(11):1523–1572.
21. Dostál Z, Horák D. Theoretically supported scalable FETI for numerical solution of variational inequalities. SIAM J Numer Anal. 2007;45(2):500–513.
22. Pechstein C. Finite and boundary element tearing and interconnecting solvers for multiscale problems. Heidelberg, Germany: Springer, 2013.
23. Klawonn A, Rheinbach O. A parallel implementation of dual-primal FETI methods for three dimensional linear elasticity using a transformation of basis. SIAM J Sci Comput. 2006;28(5):1886–1906.
24. Li J, Widlund OB. FETI-DP, BDDC, and block Cholesky method. Int J Numer Methods Eng. 2006;66:250–271.
25. Stewart GW. Matrix algorithms, vol. I, Basic decompositions. Philadelphia: SIAM, 1998.
26. Ipsen IC, Mayer CD. The angle between complementary subspaces. Am Math Mon. 1995;102(10):904–911.
27. Mayer CD. Matrix analysis and applied linear algebra. Philadelphia: SIAM, 2000.
28. Golub GH, Van Loan CF. Matrix computations. 4th ed. Baltimore: John Hopkins University Press, 2012.
29. Horn RA, Johnson CR. Topics in matrix analysis. Cambridge, MA: Cambridge University Press, 1991.
30. Schacke K. On the Kronecker product [MSc. thesis], University of Waterloo; 2004.
31. ESPRESO - Highly parallel framework for engineering applications. <http://numbox.it4i.cz>.
32. Dostál Z, Kozubek T, Vlach O. Reorthogonalization based stiffness preconditioning in FETI algorithms with applications to variational inequalities. Numer Linear Algebra Appl. 2015;22(6):987–998.

**How to cite this article:** Dostál Z, Horák D, Brzobohatý T, Vodstrčil P. Bounds on the spectra of Schur complements of large H-TFETI-DP clusters for 2D Laplacian. *Numer Linear Algebra Appl.* 2021;28:e2344. <https://doi.org/10.1002/nla.2344>